Analytical Model and Experimental Validation of Friction Laws for Composites Under Low Loads

Olga Smerdova, Juliette Cayer-Barrioz, Alain Le Bot, Boris Sarbaev

Tribol Lett
DOI 10.1007/s11249-012-9947-2

ORIGINAL PAPER

Analytical Model and Experimental Validation of Friction Laws for Composites Under Low Loads

O. Smerdova · J. Cayer-Barrioz · A. Le Bot · B. Sarbaev

Received: 27 January 2012 / Accepted: 9 March 2012

Abstract In order to account for interfacial friction of composite materials, an analytical model based on contact geometry and local friction is proposed. A contact area includes several types of microcontacts depending on reinforcement materials and their shape. A proportion between these areas is defined by in-plane contact geometry. The model applied to a fibre-reinforced composite results in the dependence of friction on surface fibre fraction and local friction coefficients. To validate this analytical model, an experimental study on carbon fibre-reinforced epoxy composites under low normal pressure was performed. The effects of fibre volume fraction and fibre orientation were studied, discussed and compared with analytical model results.

Keywords Unlubricated friction · Interfacial friction · Composite · Carbon, graphite · Polymers (solids)

1 Introduction

In 1978, Briscoe and Tabor [1] explained that for solid polymer friction, the frictional force, T, arises from energy dissipation in two regions: interfacial and bulk. The processes occurring in these two regions are of different natures and described by distinct terms. The interfacial region friction is characterised by interfacial shear strength, τ, acting on the real contact area, A. The main condition of interfacial friction is the absence of material transfer, which implies a weak normal loading. The thickness of this interfacial zone for organic polymers is between 10 and 100 nm [2]. The real area of contact for low loads could be calculated by means of the non-adhesive Hertz elastic contact theory [3], or adhesion Johnson–Kendal–Roberts [4] or Derjaguin–Muller–Toporov [5] solutions.

The term 'interfacial friction' as an opposite to the classical, wear accompanied, friction was also introduced by Homola et al. [6]. This is the friction which occurs during the sliding of two perfect, molecularly smooth, undamaged surfaces, either in molecular contact or separated by molecularly thin films of liquid or lubricant fluids. The two surfaces do not come into true molecular contact, but remain separated by a distance of a few angströms. This requires a short-range repulsive force between the surfaces and a low applied load. Homola et al. have found from experiments on mica, that, in agreement with Johnson–Kendal–Roberts adhesive friction theory, the friction is proportional to the contact area, which shows no proportionality to the load especially at small and negative loads. Another friction regime appears when damage occurs and propagates rapidly, the friction becomes proportional to the normal load and obeys Amontons' first law: $T = \mu N$. According to this theory, the critical shear stress, being a function of the surface energy, surface or asperity radii, elastic modulus and external load, is the sum of internal, external and elastic contributions.

Myshkin et al. [7], studying polymer friction, notice that the surface and cohesion forces are nearly equal, and fracture often occurs in the bulk. Their vast literature review shows that the friction coefficient remains practically constant until a critical load, although the width of the range of this load depends on the polymer type

A1 O. Smerdova (✉) · J. Cayer-Barrioz · A. Le Bot
A2 LTDS—UMR5513 CNRS, Ecole Centrale de Lyon, 36 Avenue
A3 Guy de Collongue, 69134 Ecully Cedex, France
A4 e-mail: olga.smerdova@ec-lyon.fr

A5 O. Smerdova · B. Sarbaev
A6 Bauman Moscow State Technical University, Moscow, Russia

Journal : Large 11249 | Dispatch : 19-3-2012 | Pages : 10
Article No. : 9947 | ☐ LE | ☐ TYPESET
MS Code : TRIL2022 | ☑ CP | ☑ DISK

(15–100 N). With regards to the velocity effect on polymer friction, it remains unclear and it is narrowly connected to the temperature rise in the contact, because polymer mechanical behaviour changes significantly with temperature.

Wear-accompanied friction of polymer composites is the subject of many experimental studies. For instance, tribological behaviour of carbon fibre/epoxy composite under Vickers indenter scratching tests [8, 9] or abrasive wear conditions [10], as well as effects of wear debris presence [11, 12], counterface material [13, 14] or temperature [15] have been studied.

The problem of polymer composite friction is usually covered by polymer friction theories. In practice, the friction coefficient, as well as the Young modulus, shear modulus or Poisson's ratio, is calculated with a rule of mixture. The idea is to represent the friction of composite material as a 'composite' friction, i.e. a linear combination of each component contributions. For the friction coefficient of fibre-reinforced composite materials, the following semi-empirical rule of mixture [16] is proposed

$$\frac{1}{\mu} = \frac{V_f}{\mu_f} + \frac{V_m}{\mu_m} \tag{1}$$

where V_f and V_m are the fibre and matrix volume fractions, μ_f and μ_m are the friction coefficients of fibre and matrix materials, respectively.

In the context of composites abrasive friction, another relationship for friction coefficient calculation was presented by Axén et al. [17–19]. The composite friction is a combination of two regimes: equal normal pressure distribution and equal wear rate distribution between the phases of the composite. However, in the case of negligible or no wear, the first regime dominates and the friction coefficient may be found as

$$\mu = \alpha_f \mu_f + \alpha_m \mu_m \tag{2}$$

α_f and α_m are fibre and matrix surface fractions, respectively.

Both Eqs. (1) and (2), as well as quoted experimental works [8–15], describe the friction between composite and non-composite, uniphase material.

Therefore, the aim of this study is to contribute to the understanding of composite friction in terms of its interfacial component with uniphase and composite counterbodies. In contrast to the previous theoretical and experimental studies, change in the bulk or damage of both surfaces are negligible. Thus, this study is dedicated to the interfacial zone between two composites.

This paper is organized into two major sections, which present the theoretical and experimental work, with a last section discussing results and conclusions. The first major section presents an analytical investigation of composite contact with a uniphase material or another composite, based on geometric consideration. The second major section describes an experimental study with unidirectional carbon fibre-reinforced epoxy materials of different fibre volume fraction under light tribological conditions. The last section discusses possible ways of application of the analytical model and the correlation between theoretical and experimental results.

2 A Geometrical Model for Interfacial Friction

2.1 Friction Laws

The proposed model is based on Bowden and Tabor [20] adhesion model of friction and the multi-materials nature of contact between two composites as shown in Fig. 1. During sliding, the contact area is renewed continuously, but its composition, i.e. the proportion between the composite components in the contact remains constant. This assumption relies on the non-occurrence of damage at the interface, which could rarefy a component by removing matter.

Therefore, the following hypothesis are imposed:

- wearless and damageless friction
- Coulomb friction for all microscopic contact spots
- uncorrelated friction forces for all microscopic contact spots
- isotropic friction for any couple of components in contact

According to Bowden and Tabor adhesion friction model, the contact of two solids is composed of a multitude of microcontacts forming a real contact area. External normal and tangential forces are distributed over these microcontacts. Since the real area of contact is much lower than the apparent one, the local stresses arising in the microcontacts exceed the yield stress and the hardest asperity penetrates into the softest one. Thus, the normal load for a composite contact, which includes several materials couples refered by the subscript i (see Fig. 2), is

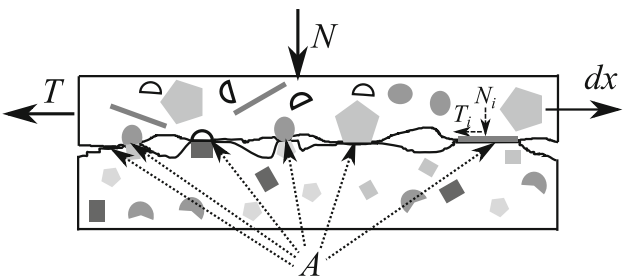

Fig. 1 Real contact area A of two sliding multiphase rough bodies in dx direction under the normal load N inducing the friction force T

Journal : Large 11249 Dispatch : 19-3-2012 Pages : 10
Article No. : 9947 LE TYPESET
MS Code : TRIL2022 CP DISK

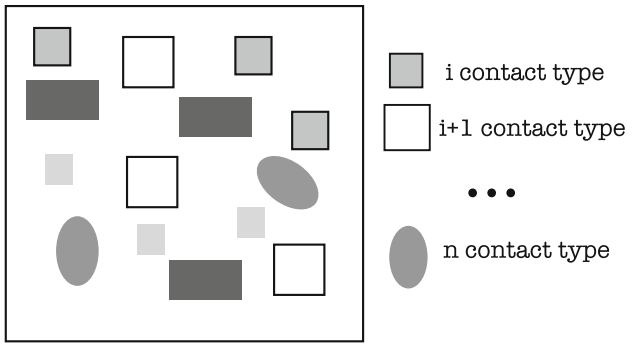

Fig. 2 Populations of microcontacts

$$N = \sum_i N_i = \sum_i H_i A_i \tag{3}$$

where H_i is the hardness of the softest material in couple i, A_i is the total contact area for all i-type contact spots.

The asperities of two materials under the normal load form the junctions. The shear stress arises in the contact until a critical value, when rupture occurs and the sliding starts.The frictional force is a product of this critical shear stress τ_i and the contact area A_i for each materials couple

$$T = \sum_i T_i = \sum_i \tau_i A_i \tag{4}$$

According to the Amontons first friction law, the friction coefficient for the composite contact may be written as follows:

$$\mu = \frac{T}{N} = \frac{\sum_i \tau_i A_i}{\sum_i H_i A_i} \tag{5}$$

A direct application of this equation is complicated because of the lack of information about real contact area and shear stresses. That is why the two special cases with an additional assumption are considered below.

Case 1: The hardness of the materials in contact is assumed to be equal to an effective hardness, i.e. $H_i = H^*$. Therefore, by taking Eq. (5) and considering that the total real area is $\sum A_i = A$,

$$\mu = \frac{T}{N} = \sum_i \frac{\tau_i}{H^*}\frac{A_i}{A} = \sum_i \alpha_i \mu_i \tag{6}$$

where $\mu_i = \tau_i/H^*$ is the friction coefficient of i-type materials couple. The contribution coefficient α_i is a surface fraction of all i-type contacts with respect to the total real area of contact between two composites.

Case 2: Another assumption is an equal effective shear stresses for all junctions of all materials couples $\tau_i = \tau^*$. Thus, Eq. (5) reduces to the inverse proportion for the composite friction coefficient:

$$\frac{1}{\mu} = \frac{N}{T} = \sum_i \frac{H_i}{\tau^*}\frac{A_i}{A} = \sum_i \alpha_i \frac{1}{\mu_i} \tag{7}$$

where $\mu_i = \tau^*/H_i$ is the friction coefficient for a couple of materials in i-type contact.

A priori this model can be applied to the contact of composites of any nature, i.e. reinforced by any type, shape and number of fillers at the condition they are uniformly distributed in the bulk.

To conclude this section, the simplified Bowden and Tabor's model applied to a multiphase contact reduces to one of two composite frictional laws: the proportionality law in Eq. (6) and the inverse proportionality law in Eq. (7). In both cases, the composite friction coefficient depends only on the partition of contact between phases of two composites and the local friction coefficient between them.

2.2 Fibre Surface Fraction: FRP Geometry

In both Eqs. (6) and (7), the question of composite friction requires the knowledge of surface fractions α_i of i-type contacts. In this study, a composite reinforced with unidirectional long fibres is considered. The contact plane is a cut parallel to the fibre direction. Before an analysis of the contact between two composite samples, a preliminary step is to calculate the surface fraction α_f of fibres in the cut plane. However, a fibre percentage in composite is usually described by the fibre volume fraction, V_f. Therefore, the question of this section is: What is the relationship between V_f, an industrial input parameter, and α_f, an output finished material characteristic?

There are several approaches to the modelling of fibre-reinforced polymer, represented by two major groups: probabilistic, which uses random fibre distribution [21, 22], and deterministic, which deals with a representative volume element conception [23].

In this work, a random uniform fibre distribution with round fibres of a constant diameter is chosen. Figure 3 shows a cubic element of size a cut out of the composite and filled with matrix and fibres of radius R. A cutting

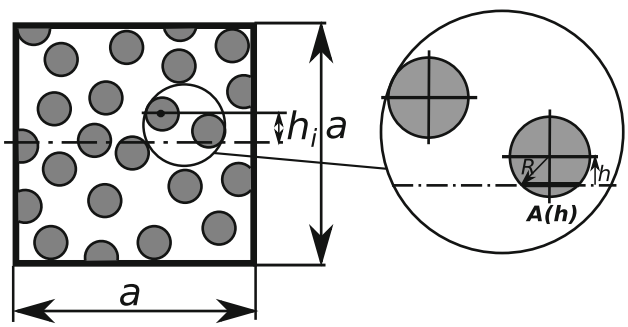

Fig. 3 Random fibre distribution in the square volume of composite of size a. $A(h)$ is the chord of the cut fibre i with the radius R, whose centre location is given by the height from the square middle h_i

Journal : Large 11249 Dispatch : 19-3-2012 Pages : 10
Article No. : 9947 LE TYPESET
MS Code : TRIL2022 CP DISK

plane, parallel to the fibre direction, separates this volume into two equal parts. The relative location of i fibre with respect to this plane is given by its height h_i. Since the fibres are assumed to be uniformly randomly distributed in the volume, the density probability function $p(h)$ is equal to

$$p(h) = \frac{1}{a},\ if\ h \in \left[-\frac{a}{2};\frac{a}{2}\right] \tag{8}$$

The middle plane cuts each fibre through a chord $A(h)$, whose length depends on the height h by

$$A(h) = \begin{cases} 2\sqrt{R^2 - h^2}, & \text{if } h \in [-R;R]; \\ 0, & \text{otherwise.} \end{cases} \tag{9}$$

The expectation of the chord for any fibre from volume a^3 is calculated from Eqs. (8) and (9) as follows:

$$\langle A(h)\rangle = \int_{-a/2}^{a/2} A(h)p(h)\mathrm{d}h = \frac{\pi R^2}{a} \tag{10}$$

The fibre surface fraction α_f is the sum of all chords $N\langle A\rangle$, where N is the total number of fibres in the volume, divided by the side a of the cutting plane

$$\alpha_f = \frac{N\langle A\rangle}{a} = \frac{N\pi R^2}{a^2} \tag{11}$$

Since the fibre volume fraction V_f for the volume a^3 is the ratio of the sum of all fibre sections $N\pi R^2$ enclosed in this volume and the square area a^2, obviously

$$\alpha_f = V_f \tag{12}$$

Hereby using the probabilistic approach, it is proved that for a uniform random distribution of fibres in a unidirectional fibre-reinforced composite, the fibre surface fraction is equal to the fibre volume fraction.

2.3 Case of FRP/Uniphase Material Contact

First application of this model is the contact of a fibre-reinforced composite with a non-composite homogeneous material. Composition of the apparent contact area in this case is shown in Fig. 4a. Two types of contact are distinguished: fibre/counterface material and matrix/counterface material. In this simple case, designating subscripts f, m and c, respectively, for fibre, matrix and counterface material, the contribution coefficients of each contact type will be equal:

$$\begin{cases} \alpha_{fc} = d_f/a = \alpha_f \\ \alpha_{mc} = d_m/a = 1 - \alpha_f \end{cases} \tag{13}$$

where d_f is the fibre diameter and d_m is the distance between two adjacent fibres.

Therefore from Eqs. (6), (7) and (13) composite friction coefficient can be calculated with one of following equations:

$$\mu = \alpha_f\mu_{fc} + (1 - \alpha_f)\mu_{mc} \tag{14}$$

if we adopt a proportionality law, and

$$\frac{1}{\mu} = \frac{\alpha_f}{\mu_{fc}} + \frac{1 - \alpha_f}{\mu_{mc}} \tag{15}$$

if we adopt an inverse proportionality law. Where μ_{fc} and μ_{mc} are friction coefficients between fibre and counterface materials and matrix and counterface materials, respectively, which are supposed to be obtained experimentally for each couple of materials.

One can notice that Eq. (14) is similar to Eq. (2) quoted in the introduction, and Eq. (15) has a similar form to Eq. (1) substituting V_f by α_f.

2.4 Case of FRP/FRP Contact

A more complex case is the contact between two equivalent FRP composites, as drawn in Fig. 4b. In this case, four types of contact are distinguished: fibre/fibre, fibre/matrix, matrix/fibre and matrix/matrix. As two composites are identical and $\mu_{fm} = \mu_{mf}$, the friction coefficient becomes equal to one of the following equations

$$\mu = \alpha_{ff}\mu_{ff} + 2\alpha_{fm}\mu_{fm} + \alpha_{mm}\mu_{mm} \tag{16}$$

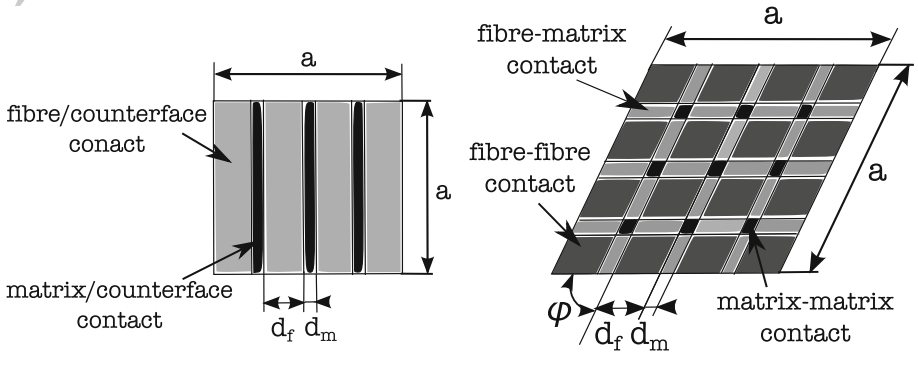

Fig. 4 Apparent contact of size $a \times a$, composed of several materials. **a** Contact between an uniphase material and a FRP with fibre diameter d_f and distance between fibres d_m. **b** Contact between two similar FRP with an angle ϕ between fibre directions of two composites

Journal : Large 11249 Dispatch : 19-3-2012 Pages : 10
Article No. : 9947 LE TYPESET
MS Code : TRIL2022 CP DISK

for the proportionality law and,

$$\frac{1}{\mu} = \frac{\alpha_{ff}}{\mu_{ff}} + \frac{2\alpha_{fm}}{\mu_{fm}} + \frac{\alpha_{mm}}{\mu_{mm}} \quad (17)$$

for the inverse proportionality law.

In order to calculate contribution coefficients α_{ff}, α_{fm} and α_{mm}, the contact is examined. The area of each apparent individual microcontact A_{ff}, A_{fm}, A_{mm} and total area A is equal to

$$A_{ff} = \frac{d_f^2}{\sin\phi}; A_{fm} = \frac{d_f d_m}{\sin\phi}; A_{mm} = \frac{d_m^2}{\sin\phi}; A = \frac{a^2}{\sin\phi} \quad (18)$$

where ϕ is the angle of orientation between the fibres of two composites. Thus, the contribution coefficients are equal to

$$\begin{cases} \alpha_{ff} = \alpha_f^2 \\ \alpha_{fm} = \alpha_f(1-\alpha_f) \\ \alpha_{mm} = (1-\alpha_f)^2 \end{cases} \quad (19)$$

Substituting Eq. (19) in Eqs. (16) and (17), two expressions for friction coefficient are obtained:

$$\mu = \alpha_f^2\mu_{ff} + 2\alpha_f(1-\alpha_f)\mu_{fm} + (1-\alpha_f)^2\mu_{mm} \quad (20)$$

for the proportionality law and,

$$\frac{1}{\mu} = \frac{\alpha_f^2}{\mu_{ff}} + \frac{2\alpha_f(1-\alpha_f)}{\mu_{fm}} + \frac{(1-\alpha_f)^2}{\mu_{mm}} \quad (21)$$

for the inverse proportionality law.

It should be noticed that this calculation reveals an independence of interfacial friction with the orientation of fibres or their diameter. The resulting curves for FRP/uniphase material and FRP/FRP contacts are presented in continuous line in Fig. 8a, b and discussed in Sect. 4 of this paper.

3 Experimental Study

The experimental validation of the proposed analytical model has been carried out on carbon fibre-reinforced epoxy composites.

The carbon or graphite is known to have particularly low friction coefficient due to its planar structure. The planes of graphene, one-atom thick smooth layers of honeycomb lattice of carbon atoms, being aligned along the fibre axis and constituting a carbon fibre surface, develop low attractive forces between each other causing a lubrication effect by delamination [24]. This effect, along with an improvement of mechanical characteristics, is appreciated for the reinforcement of polymer composites, which gives them the name self-lubricated [25]. Therefore, graphite additives are commonly used in tribological polymer applications, as for instance in journal bearings [26], gears [27] or space structures [28, 29]. However, different forms of carbon currently used to reinforce polymers—such as aligned long fibres, randomly dispersed chopped fibres, nanotubes, nanoparticles, powder or graphite flakes—result in various tribological behaviors.

Two aspects are of interest in this study: the effect of the fibre volume fraction and the influence of the fibre orientation on friction coefficient. The latter was the object of previous studies [30–33], which revealed a significant effect of fibre orientation on the friction coefficient of carbon fibre/epoxy composites under rather severe sliding conditions causing wear.

In contrary to the above-mentioned works, specific attention is consecrated to ensure tribological conditions excluding surface damage in this study.

3.1 Materials

Two types of specimen geometry have been designed: a fixed rectangular sample of 80 × 25 × 5 mm referred to as the track, and a round sample ø20 × 5 mm sliding over the track. The composite materials differ by fibre volume fraction: 0 %, i.e. pure epoxy HexPly® M10.1, 34, 52 and 62 % of carbon fibres. The latter is a unidirectional carbon fibre-reinforced epoxy made up from prepreg plies HexPly® M10/ 38 %/UD300/CHS. The two intermediate composites contain layers of carbon fibres HexTow AS4, aligned in one direction and integrated into the epoxy resin HexPly® M10.1. However, out-of-plane alignment of fibres is not controlled, therefore the surfaces of 34 and 52 % samples are strongly heterogeneous and expose pure epoxy zone and some zones of carbone fibre hanks as shown in Fig. 5.

All the rubbing surfaces were polished successively with abrasive papers *P*600, *P*2400 and *P*4000 from seconds to minutes depending on initial surface state. The profile characteristics for the polished samples of four fibre percentages are presented in Table 1. Before each experiment, both surfaces are carefully cleaned with heptane, acetone and propanol-2 successively and finally with a flow of nitrogen.

3.2 Experimental Set-up

The experiments have been carried out on the tribometer RA [34], a scheme of which is drawn in Fig. 6. The tribometer allows one to perform a linear reciprocated motion between two planes of relatively large surfaces and to measure simultaneously the friction force induced by sliding. The specificity of this tribometer is to provide a low contact pressure. The normal force is applied by means of a weight put onto the slider (up to 20 N). A brushless servomotor (type Danaher AKM22C) guides the motion of the lever pushing the upper sample. The rotating velocity

Journal : Large 11249 Dispatch : 19-3-2012 Pages : 10
Article No. : 9947 LE TYPESET
MS Code : TRIL2022 CP DISK

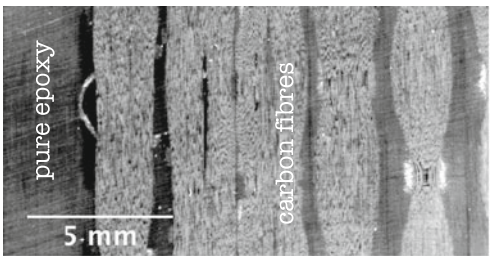

(a)

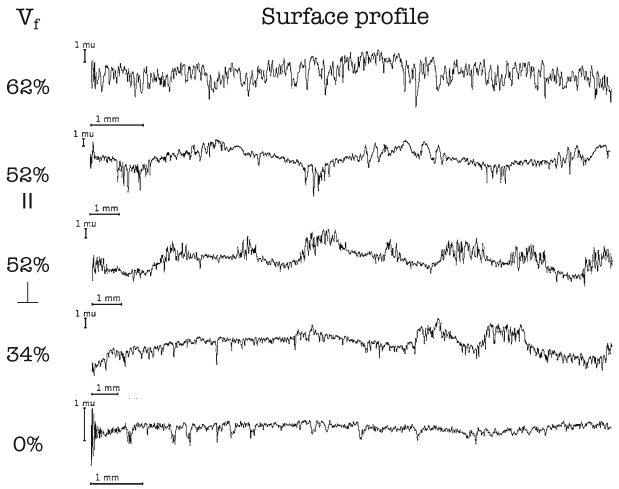

(b)

Fig. 5 Sample surfaces. **a** Photo of 34 % sample rubbing surface with pure epoxy zones and carbon fibre hanks. **b** Surface profiles for pure epoxy and 34, 52 and 62 % of fibre volume fractions composites. The periodic bumps on the surface of 34 and 52 % correspond to the exposed fibre hanks

Table 1 Surface characteristics of track samples based on 5 measurements for each sample (ISO4287)

Fibre volume fraction V_f (%)	Arithmetic roughness *Ra* (μm)	Quadratic roughness *Rq* (μm)
0	0.05 ± 0.01	0.07 ± 0.01
34	0.50 ± 0.24	0.75 ± 0.44
52	0.27 ± 0.07	0.35 ± 0.09
62	0.36 ± 0.10	0.45 ± 0.12

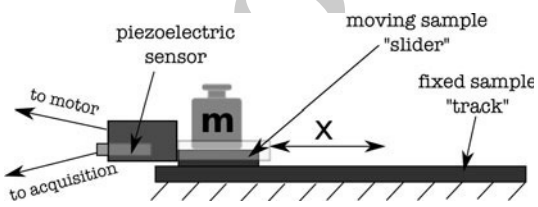

Fig. 6 Principle of the tribometer *RA*

of the motor is measured by a decoder and is maintained constant by a feedback loop with electrical variator (Servostar 300), whose accuracy is 1 %. The resulted range of velocity for the lever is from few μm/s to 2 m/s. During an experiment, the tangential force is continuously measured by KISTLER Type 9217A piezoelectric sensor (stiffness $\approx 15\ N/\mu m$, range force from −50 to 50 N, sensitivity $\approx -98.5 \times 10^{-12}$ C/N) fixed in the lever. Before its acquisition with a sampling frequency 1 kHz, the signal is amplified by a KISTLER Type 5018A charge amplifier (for the force range of −50 to 50 N, gain is 5 N/V).

3.3 Experimental Conditions

The ambient humidity (RH ≈50–60 %) and room temperature (T ≈20–25 °C) were measured during each experiment. A preliminary study showed that the variation of sliding velocity from 0.1 to 200 mm/s and normal load from 0.1 to 20 N does not influence the friction coefficient between two CFRP. However, in order to compare fairly the friction of different materials, the normal load is maintained constant at about 0.5 N, which corresponds to the mean apparent contact pressure of 1.56 kPa, in order to avoid considerable wear and bulk deformation, which were observed in the case of pure epoxy samples under higher normal load. The fibre orientation effect tests were carried out under the normal load of 10 N corresponding to 31.2 kPa on the samples of 62 % of fibres. Each test consists of 50 cycles. The summary of experimental conditions is presented in Table 2. Each couple of materials has been tested at least ten times.

The instantaneous friction coefficient is defined as the ratio of a tangential force and a constant normal force. The friction coefficient discussed below is the kinetic one.

3.4 Experimental Results

Epoxy/epoxy, composite/epoxy and composite/composite friction experiments were carried out to identify the fibre content effect and to validate the theoretical model conclusions. An example of the first cycles for composite/composite and epoxy/epoxy couples is presented in Fig. 7 and reveals a relatively stable frictional force during each cycle and for the whole test in both cases. After each experiment, the surfaces were observed in order to verify the absence of surface damage. It was concluded that chosen experimental conditions are favourable for wearless friction.

Table 2 Experimental conditions

Motion type	Velocity (mm/s)	Sliding distance (mm)	Normal load (N)	Apparent contact area (mm^2)
Linear reciprocating	10	60	0.5–10	314

Journal : Large 11249 Dispatch : 19-3-2012 Pages : 10
Article No. : 9947 LE TYPESET
MS Code : TRIL2022 CP DISK

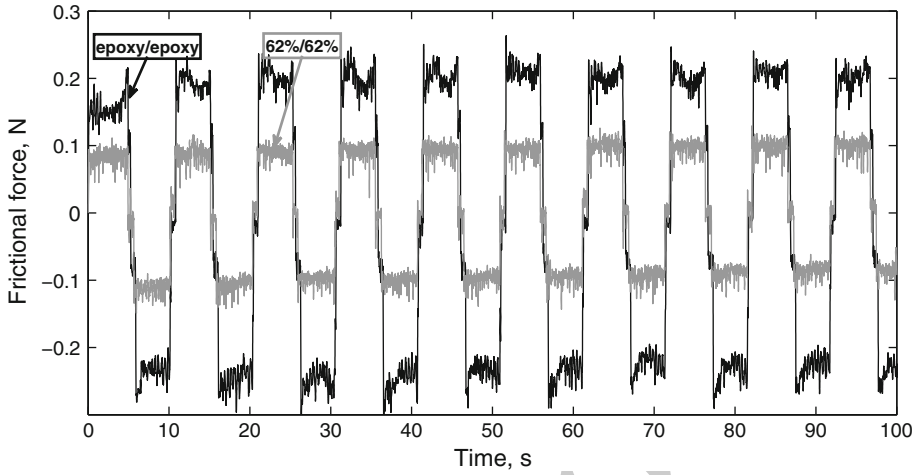

Fig. 7 Evolution of the frictional force versus time for epoxy/epoxy and composite/composite ($N = 0.5$ N, corresponding to a contact pressure $p = 1.56$ kPa; $V = 10$ mm/s)

Figure 8a, b presents the results for all pairs in terms of kinetic friction coefficient versus fibre volume fraction of two samples in contact. A wide dispersion of friction coefficients for all experiments with pure epoxy and the values of 0.4 ± 0.07 for epoxy/epoxy and 0.45 ± 0.06 for epoxy/composite couples were observed. However, in the case of composite/composite couple, the value of friction coefficient was significantly lower and slightly varied for all test conditions: 0.17 ± 0.01. The wide dispersion of friction coefficient when epoxy is used might be related to the humidity influence [35].

In order to verify the independence of friction coefficient on fibre orientation in the case of composite/composite contact as concluded from the analytical model, experiments between 62 %/62 % composites were carried out. The friction coefficient versus the total angle between fibre orientations of two samples, ϕ, is shown in Fig. 9. It was found that between two limit cases: $\phi = 0°$—the fibres of two samples are oriented parallel to the sliding direction, and $\phi = 180°$—both are perpendicular to the sliding direction, the friction coefficient for interfacial sliding conditions changes slightly from 0.16 to 0.17.

4 Discussions and Conclusions

4.1 Validation of the Theoretical Laws

The theoretical model proposed in this paper is based on the differentiation of each composite phase contact with counterface material, both to composite and uniphase material. In order to verify the theoretical model conclusions, its application to carbon fibre/epoxy composite in contact with either pure epoxy or fibre composite is discussed in this section.

As it was shown in Sect. 2, in order to predict the friction coefficient between two carbon fibre-reinforced epoxy composites as well as for its contact with pure epoxy, three values of friction coefficients (carbon fibre/carbon fibre, carbon fibre/epoxy and epoxy/epoxy) are required.

Whereas the epoxy/epoxy friction coefficient is measured in this study and its average value is equal to 0.4, the experiments of friction between carbon fibres were carried out by Roselman and Tabor in 1976–1977 [36, 37]. They rubbed individual carbon fibres of two types (high strength and high modulus) with and without surface treatment against each other under normal load in the range of order 10^{-8} to 10^{-2} N, and against other materials, including epoxy, under normal load in the range of order 10^{-4} to 10^{-2} N. A great effect of normal force on the carbon fibre friction was observed. The friction of high strength fibres is two times higher than for high modulus fibres.

The summary of the values used in Eqs. (14) and (15); Eqs. (20) and (21) derived from the theoretical model is presented in Table 3. The values for high strength carbon fibres, similar to those used in the present experimental study, were chosen. Figure 8a, b presents a comparison of the proposed analytical model using the values from Table 3 and the experimental results. The friction coefficients are plotted versus fibre volume fraction for the experimental results and versus fibre surface fraction for the analytical results. Their equality, proved in Sect. 2.2, permits us to put them on the same abscissae axis.

It is seen from Fig. 8a that average values of friction coefficients observed experimentally for CFRP/epoxy couples fit to both theoretical curves, plotted according to Eqs. (14) and (15), rather well. Beside the validation of composite/uniphase material friction laws, this can be interpreted such as the values of epoxy/epoxy and carbon fibres/epoxy friction coefficients measured for individual materials [36, 37] might be applied to calculate the composite one, and the hypothesis of uncoupled friction contributions of each component is credible.

Journal : Large 11249 | Dispatch : 19-3-2012 | Pages : 10
Article No. : 9947 | LE | TYPESET
MS Code : TRIL2022 | CP | DISK

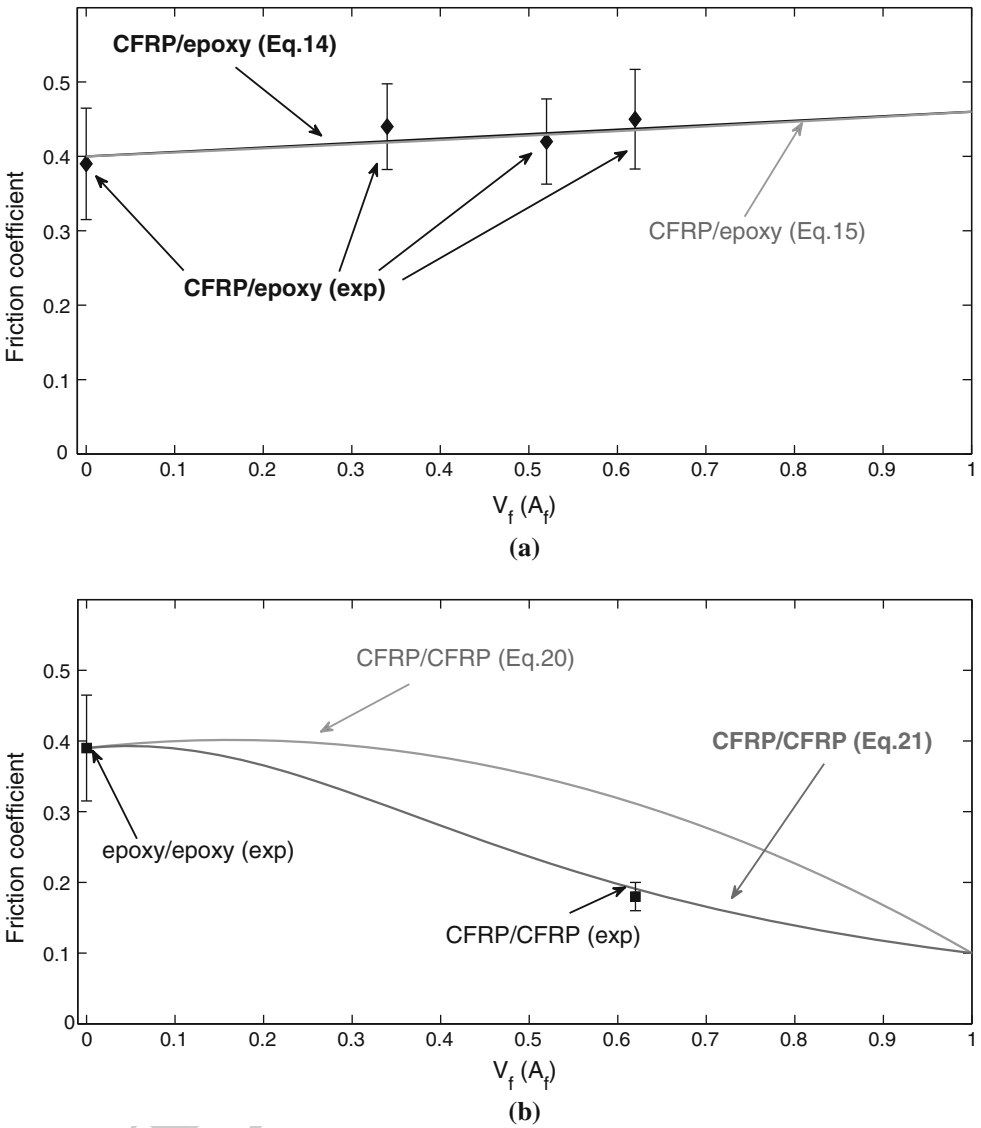

Fig. 8 Experimental (*black points* with *error bars*) and theoretical (*grey lines*) results corresponding to Eqs. (14) and (15) in case of composite/epoxy contact (**a**), and Eqs. (20) and (21) in case of composite/composite contact (**b**) calculated with values from Table 3. **a** FRP/uniphase. **b** FRP/FRP

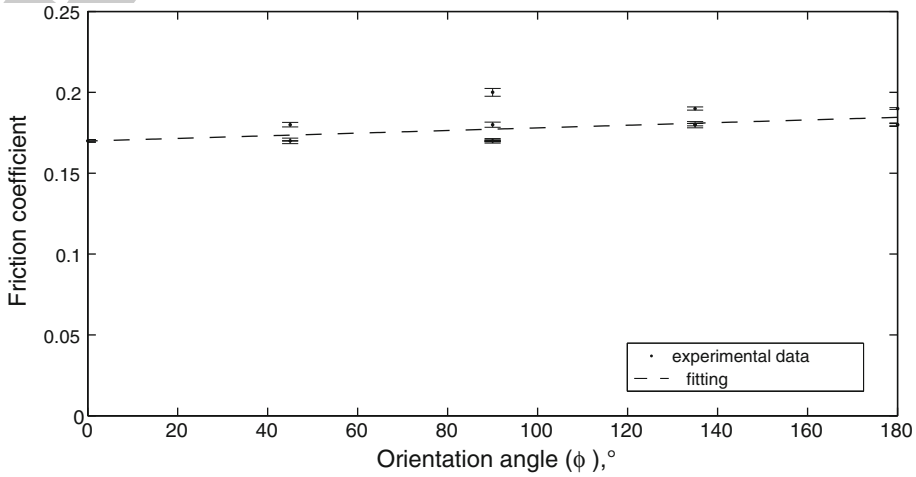

Fig. 9 Experimentally measured kinetic friction coefficients versus total angle between fibre orientations of two samples (pressure 1.56 kPa, sliding velocity $V = 10$ mm/s)

Journal : Large 11249 Dispatch : 19-3-2012 Pages : 10
Article No. : 9947 LE TYPESET
MS Code : TRIL2022 CP DISK

Table 3 Local friction coefficients

Normal load	10^{-5} to 10^{-2} N	10^{-3} N	2 N
Materials	Carbon fibre HS/ carbon fibre HS	Epoxy/carbon fibre HS	Epoxy/ epoxy
Friction coefficient	0.7–0.1 [36]	0.46 [37]	0.4

The carbon fibre/carbon fibre friction coefficient of 0.1, along with values for epoxy/epoxy and carbon fibre/epoxy used for previous case, were substituted in Eqs. (20) and (21). Two result curves and one experimental point for the 62 %/62 % are plotted in Fig. 8b. One can certify, that the inverse proportionality law curve passes through the experimental point.

The fact that the inverse proportionality law Eq. (7) fits better the experimental results for composite/composite friction, and both Eqs. (6) and (7) are applicable for epoxy/composite friction, has an explanation, which could validate the assumptions about effective hardness H^* and effective shear stress τ^*. Indeed, in the case of epoxy/composite contact, the hardness used in Eq. (6) is similar for epoxy/epoxy and epoxy/carbon contacts, because this is the softest material, i.e. epoxy, hardness. Shear stresses for these two contact types, which can be found as $\tau_i = \mu_i H_i$, are also rather similar because of a closeness of their friction coefficients.

The composite as a counterface material adds carbon/carbon contact to the zones discussed above. The hardness of carbon fibres is about ten times higher than that of epoxy [38], while the friction coefficient between carbon fibres is much lower than the friction coefficients of epoxy/epoxy and epoxy/carbon contacts. Thus, shear stresses, calculated with $\tau_i = \mu_i H_i$, must be of the same order for these three contact types. This explains why Eq. (7) is better for composite/composite friction.

4.2 Discussions and Perspectives

Although this model fits rather well experimental results, we propose some useful ideas to improve it in this section. At least two factors, which have not been considered in this model, could affect a partition of composite contact between its phases. The first is a surface profile. As seen in Fig. 5, the composite materials are rougher than the pure polymer, even if they were polished following a similar procedure. In the case of 52 %, it is clear that only fibre locks are exposed to the contact. It is supposed that the asperities of both surfaces are deformed under normal load, but the magnitude of this deformation for different phases is unknown. Hence, a second important factor of contact area distribution is normal pressure partition between phases. It is likely that matrix carries less of the load than reinforcement due to the difference in rigidity. The idea of composite friction coefficient depending on the load carried by each composite phase and friction coefficients between these phases was proposed by Schön [39], who made the experiments with wear-accompanied friction between CFRP, resulting in the following equation:

$$\mu = \frac{1}{P}\left(\mu_{\mathrm{mm}} P_{\mathrm{mm}} + \mu_{\mathrm{fm}} P_{\mathrm{fm}} + \mu_{\mathrm{ff}} P_{\mathrm{ff}}\right) \tag{22}$$

Therefore, we can suppose that the real contribution of each contact type is a combination of geometrical, profile and load factors.

Other important problem is the relationship between surface and volume fractions of each phase, which is roughly solved for the fibre-reinforced composite case by a probabilistic approach, but could not been estimated for the general case of any composite material. Along with theoretical calculations, some methods based on microscopic observation might be used for this purpose, for instance TEM particle density, Morsita's Index or Skewness–Quadrat Method [40]. A comparison of different methods with an evaluation of the general one applicable to any composite material along with a study of pressure distribution influence should be the object of a future research.

Acknowledgments This study was financed by the Ministry of Foreign Affairs, The Service of Cooperation for the Science, Technology and Space of the Embassy of France as well as by the Rhone-Alpes Region of France.

References

1. Briscoe, B.J., Tabor, D.: Friction and wear of polymers: the role of mechanical properties. Br. Polym. J. **10**, 74–78 (1978)
2. Briscoe, B.J.: Friction of organic polymers. In: Singer, I.L., Pollock, H.M. (eds) Fundamentals of Friction: Macroscopic and Microscopic Processes. pp. 167–182. Kluwer Academic Publishers, Dordrecht (1992)
3. Landau, L.D., Lifshitz, E.M.: Theory of elasticity. Volume 7 of course of theoretical physics. Pergamon Press, Oxford (1959)
4. Johnson, K.L., Kendall, K., Roberts, A.D.: Surface energy and the contact of elastic solids. Proc. R. Soc. Lond. A **324**, 301–313 (1971)
5. Derjagin, B.V., Muller, V.M., Toporov, Yu.P.: Effect of contact deformations on the adhesion of particles. J. Colloid Interface Sci. **53**, 314–326 (1971)
6. Homola, A.M. et al.: Fundamental experimental studies in tribology: the transition from interfacial friction of undamaged molecularly smooth surfaces to normal friction with wear. Wear **136**, 65–83 (1990)
7. Myshkin, N.K. et al.: Tribology of polymers: adhesion, friction, wear and mass-transfer. Tribol. Int. **38**, 910–921 (2005)
8. Liang, Y.N. et al.: Effect of fiber orientation on a graphite fiber composite in single pendulum scratching. Wear **198**, 122–128 (1996)
9. Beaumont, M. et al.: Research report. Scratch testing of advanced composite surfaces. Compos. A **28A**, 683–686 (1997)

Journal : Large 11249 | Dispatch : 19-3-2012 | Pages : 10
Article No. : 9947 | LE | TYPESET
MS Code : TRIL2022 | CP | DISK

10. Cirino, M., Pipes, R.B., Friedrich, K.: The abrasive wear behaviour of continuous fibre polymer composites. J. Mater. Sci. **22**, 2481–2492 (1987)
11. Lee, H.G., Seong, S.K., Lee, D.G.: Effect of compacted wear debris on the tribological behaviour of carbon/epoxy composites. Compos. Struct. **74**, 136–144 (2006)
12. Lee, H.G., Hwang, H.Y., Lee, D.G.: Effect of wear debris on the tribological characteristics of carbon fiber epoxy composites. Wear **261**, 453–459 (2006)
13. Schön, J.: Coefficient of friction for aluminum in contact with a carbon fiber epoxy composite. Tribol. Int. **37**, 395–404 (2004)
14. Giltrow, J.P., Lancaster, J.K.: The role of the counterface in the friction and wear of carbon fibre reinforced thermosetting resins. Wear **16**, 359–374 (1970)
15. Giltrow, J.P.: The influence of temperature on the wear of carbon fiber reinforced resins. ASLE Trans. **16**(2), 83–90 (1973)
16. Stachowiak, G., Batchelor, A.W.: Engineering Tribology. Elsevier Butterworth-Heinemann, Oxford (2005)
17. Axén, N., Jacobson, S.: A model for the abrasive wear resistance of multiphase materials. Wear **174**, 187–199 (1994)
18. Axén, N., Lundberg, B.: Abrasive wear in intermediate mode of multiphase materials. Tribol. Int. **28**(8), 523–529 (1995)
19. Axén, N., Hutchings, I.M., Jacobson, S.: A model for friction of multiphase materials in abrasion. Tribol. Int. **29**(6), 467–475 (1996)
20. Bowden, F.P., Tabor, D.: The Friction and Lubrication of Solids I. Clarendon Press, Oxford (1950)
21. Povirk, G.L.: Incorporation of microstructural information into models of two-phase materials. Acta Metall. Mater. **43**(8), 3199–3206 (1995)
22. Sankaran, S., Zabaras, N.: A maximum entropy approach for property prediction of random microstructures. Acta Mater. **54**, 22652276 (2006)
23. Sun, C.T., Vaidya, R.S.: Prediction of composite properties from a representative volume element. Compos. Sci. Technol. **56**, 171–179 (1996)
24. Donnet, J.-B., Bansal, R.C.: Carbon Fibers. Marcel Dekker Inc, New York (1984)
25. Lancaster, J.K.: Polymer-based bearing material. The role of fillers and fibre reinforcement. Tribology **5**, 249–255 (1972)
26. Sliney, H.E., Jacobson, T.P.: Performance of graphite fiber-reinforced polyimide composites in self-aligning plain bearing to 315 C. NASA Technical memorandum, TM X-71667 (1975)
27. Kurokawa, M., Uchiyama, Y., Nagai, S.: Performance of plastic gear made of carbon fiber reinforced poly-ether-ether-ketone. Tribol. Int. **32**, 491–497 (1999)
28. Fusaro, R.L.: Self-lubricating polymer composites and polymer transfer film lubrication for space applications. NASA Technical memorandum 102492 (1990)
29. Voevodin, A.A., Zabinski, J.S.: Nanocomposite and nanostructured tribological materials for space applications. Compos. Sci. Technol. **65**, 741–748 (2005)
30. Tsukizoe, T., Ohmae, N.: Wear performance of unidirectionally oriented carbon-fibre-reinforced plastics. Tribol. Int. **8**, 171–175 (1975)
31. Sung, N.-H., Suh, N.P.: Effect of fiber orientation on friction and wear of fiber reinforced polymeric composites. Wear **53**, 129–141 (1979)
32. Shim, H.H., Kwon, Oh.K., Youn, J.R.: Effect of fiber orientation and humidity on friction and wear properties of graphite fiber composites. Wear **157**, 141–149 (1992)
33. Tripathy, B.S., Furey, M.J.: Tribological behaviour of unidirectional graphite-epoxy and carbon-PEEK composites. Wear **162**(164), 385–396 (1993)
34. Le Bot, A., Bou Chakra, E.: Measurement of friction noise versus contact area of rough surfaces weakly loaded. Tribol. Lett. **37**, 273–281 (2010)
35. Lancaster, J.K.: A review of the influence of environmental humidity and water on friction, lubrication a and wear. Tribol. Int. **23**(6), 371–389 (1990)
36. Roselman, I.R., Tabor, D.: The friction of carbon fibres. J. Phys. D **9**, 2517–2532 (1976)
37. Roselman, J.C., Tabor, D.: The friction and wear of individual carbon fibres. J. Phys. D **10**, 1181–1194 (1977)
38. Rubin, A.: ICS, Private Communication (2011)
39. Schön, J.: Coefficient of friction of composite delamination surfaces. Wear **237**, 77–89 (2000)
40. Kim, D., Lee, J.S. et al.: Microscopic measurement of the degree of mixing for nanoparticles in polymer nanocomposites by TEM images. Microsc. Res. Tech. **70**, 539–546 (2007)

Journal : Large 11249 | Dispatch : 19-3-2012 | Pages : 10
Article No. : 9947 | ☐ LE | ☐ TYPESET
MS Code : TRIL2022 | ☑ CP | ☑ DISK